MINISTRY OF EDUCATION AND TRAINING

VIETNAM ACADEMY OF SCIENCE AND TECHNOLOGY

GRADUATE UNIVERSITY SCIENCE AND TECHNOLOGY

Nguyễn Thị Thùy Vân

PHOTOCATALYTIC DEGRADATION OF *p*-XYLENE GASEOUS ON LOW BAND GAP THIN FILMS

Major: Inorganic Chemistry
Code: 9440113

SUMMARY OF INORGANIC CHEMISTRY DOCTORAL THESIS

HO CHI MINH CITY – 2023

The thesis was completed at Gradute University of Science and Technology- Vietnam Academy of Science and Technology.

Supervisor: Prof. Dr.Sc. Luu Cam Loc

Reviewer 1: …
Reviewer 2: …
Reviewer 3: ….

The thesis will be defended in front of the Academy- PhD Thesis Evaluation Council, at Graduate University of Science and Technology- Vietnam Academy of Science and Technology on ... hour .., date ... month … in 2023

INTRODUCTION

1. The necessity of the thesis

The living environment in the world is currently being seriously threatened by pollution from living processes and industrial production, including persistent volatile organic compounds (VOCs). The study of a highly efficient method to treat these pollutant compounds has become an urgent problem today. Recently, the study on the preparation and application of new semiconductors such as perovskite (ABO_3) and metal-organic frameworks (MOFs) as photocatalysts in pollutant treatment is of great interest. Perovskite has low bandgap energy and flexible structure, easy to be modified, while MOFs are new materials with outstanding advantages (diverse structure, large specific surface area and porosity, low band gap) which are suitable as a photocatalyst. Currently, in the field of perovskite photocatalysts $LaMO_3$ (with M being transition metals) and MOFs are studied to prepare and investigate their activity in the liquid and gas phase, but still limited. In particular, thin-film perovskite and MOF photocatalysts and reaction kinetics are still rare.

Therefore, a systematic study on the preparation, properties as well as the activity of perovskite and MOFs as the thin film photocatalysts for the degradation of VOCs (with p-xylene) is necessary to improve high efficiency in treatment, recovery and reuse of catalysts. Combining UV with visible light to improve reaction efficiency is a highly scientific approach, improving the efficiency of pollutant treatment as well creating a scientific basis for the use of sunlight. The study of reaction kinetics, on the one hand, provides important information to improve and enhance the activity of the catalyst, on the other hand, it is a bridge between basic research on catalysis and the design of reactors in industry. These studies create favorable conditions for the practical implementation of VOCs polluted gas treatment technology.

2. Scope of the Thesis

- Study on synthesis of visible light-sensitive perovskite materials $LaMO_3$ and metal-mechanical framework materials that are stable of heat and water, and high active performance for application as thin film photocatalysts under UV-visible light.

- Study and propose a kinetic model of the photocatalytic degradation of *p*-Xylene in the gas phase on typical catalysts.

3. The main contents of the thesis

- Study on synthesizing $LaMO_3$ perovskite materials (M: Mn, Fe, Co) by sol-gel method. Investigate the influence of technological factors (calcination temperature and time, reactants ratio) on material properties. Fabrication of visible light sensitive $LaMO_3$ thin film photocatalysts.

- Study and fabricate thin film photocatalysts of catalysts which are stable in heat and water environment and highly active of MOF materials (UiO66, UiO66-NH_2 and Zn-MOF-74) by solvo-thermal method and coating techniques.

-Analyzing the physicochemical properties of catalysts by advanced analytical methods (XRD, FT-IR, SEM, TEM, UV-Vis, XPS…).

- Investigate the activity of catalysts in the photooxidation of *p*-xylene in gas phase under the mixture of UV and visible light irradiation.

- Study the kinetics of the deep oxidation of *p*-xylene in gas phase on typical photocatalysts under the mixture of UV and visible light and propose kinetic equation.

CHAPTER 1. OVERVIEW

In the world, every year about 115.10^{10} kg VOCs are emitted from both natural and man-made sources. VOCs seriously affect human health even at relatively low concentrations. Currently, many methods to treat VOCs are studied and applied. There, photocatalytic oxidation using a mixture of UV light

and visible light is being interested because of its high efficiency and economy. New and diverse photocatalysts can be activated by sunlight including perovskite and MOFs are constantly being researched and discovered. The photocatalytic activity of the perovskites is easily changed when different metal elements are substituted in the structure. The photocatalytic properties of MOFs are related to the photon adsorption of organic linkers, then energy to be transferred to metal sites under ultraviolet or visible light. A remarkable feature is that compared with traditional photocatalysts, MOFs have better optical activity because they are easily to be changed the band gap energy when adding substances such as transition metals, organic functional groups such as halogens, amines, and alkyls.

Based on published research results, perovskite materials and MOFs are ideal candidates to become potential photocatalysts. However, up to now, most of the research has focused on their application as gas adsorbents or pollutant treatment in water. Study on the application of thin film catalysts based on these materials in polluted gas treatment is still limited. Therefore, the thesis focuses on preparing unpublished thin film photocatalysts from potential perovskite materials ($LaMnO_3$, $LaFeO_3$, $LaCoO_3$) and MOFs (UiO66, UiO66-NH_2, Zn-MOF-74), study on their application in photooxidation of VOCs (typically p-xylene) in the gas phase.

CHAPTER 2. METHODOLOGIES

2.1. Synthesis of perovskite $LaMO_3$ (M=Fe, Co, Mn) were prepared by the sol–gel method

$La(NO_3)_3$, $Mn(NO_3)_2.4H_2O$ (or $Fe(NO_3)_3.9H_2O$ or $(Co(NO_3)_2.6H_2O)$ and $C_6H_8O_7.H_2O$ were dissolved in a volume of 125 mL distilled water. Sol will be formed at pH 7 for 2 hrs, then will be aged in air for 24 hrs to form gel state.

2.2. Synthesis UiO66, UiO66-NH_2 và Zn-MOF-74 was synthesized by a solvothermal method

UiO66 (UiO66–NH_2): Dissolve $ZrCl_4$ and 1,4-benzendicarboxylic acid (or 0,252 g 2-aminoterephtalic) in the mixture of water and dimethylformamide (DMF). The solution was heated to 120 °C in 36 hrs.

Zn-MOF-74: Dissolve 2,5-Dihydroxybenzene-1,4-dicarboxylic acid H_4DOBDC and Zinc nitrate hexahydrate $Zn(NO_3)_2.6H_2O$ in a mixture solvent of H_2O and DMF. The mixture was heated at 100 ^{0}C for 22 hrs.

After cooling to room temperature, crystals of MOFs were obtained. Wash the crystals with DMF and CH_3OH 3 times, continuously, each 24 hrs.

2.3. Creating thin films on glass tubes

Thin film catalyst was coated on pyrex glass tubes (∅ = 19 mm, L = 270 mm), which was treated with 1M HF, by deep coating method of perovskite gel or suspensions of UiO66, UiO66-NH_2 and a mixture of Zn- MOF-74+TiO_2 P25. The mass of the catalyst film is 15 mg of catalyst/tube. After drying in the air for 20 to 24 hr, the catalyst film on the glass tube was activated in the air at 500 ^{o}C for 3 hr for $LaFeO_3$ and $LaMnO_3$; 600 ^{o}C for 2 hr for $LaCoO_3$. The MOF catalyst samples were activated under vacuum at 200 ^{o}C for 7 hr with UiO-66 and UiO-66-NH_2; 250 ^{o}C for 6 hr with Zn-MOF-74.

2.4. Catalysts characterizations

Catalyst samples were determined charateristics including phase compositions (XRD), the morphology of catalyst's surface (SEM, TEM), specific surface area and poros volumn (BET), band gap and adsorbtion light region (UV-Vis), oxidation states of elements (XPS), functional groups on catalyst's surface (FT-IR), thermal stability (TGA) and thickness of thin film by Stylus method.

2.5. Evaluation of photocatalytic performance

The photoactivity of the catalysts was investigated by the micro-flow method using two lighting modes: 1) mode I (mixed UV-vis light) including 1 UV lamp

(λ = 365 nm, power 8 W, light intensity 650 Lux) and 81 LEDs (λ = 470 nm, power 0.24 W/bulb, total light intensity 65 Lux), 2) mode II (visible light) including 176 LED lamp (λ = 470 nm, power 0.24 W/bulb, total light intensity 130 Lux. Amount of catalyst used 15 mg, illuminated catalyst surface area 130 cm^2. Total gas flow 3 L/h. The concentration of p-xylene in the feed gas mixture is 19 mg/L, the oxygen and the water vapor concentrations are varied in the investigation range. The catalyst treatment conditions are suitable as well as the best reaction conditions were selected through p-xylene conversion over reaction time (X) and p-xylene conversion efficiency after 60 min of reaction (H_{60}).

2.5.1. Analysis of the reaction mixture

The reaction mixture was analyzed on an Agilent 6890 Plus gas chromatograph (GC) (FID, DB-624 capillary column) and gas chromatography-mass spectrometer GC-MS 6890N/MSD5973 (TCD probe and HP-PlotQ capillary column).

2.5.2. Experimental diagram.

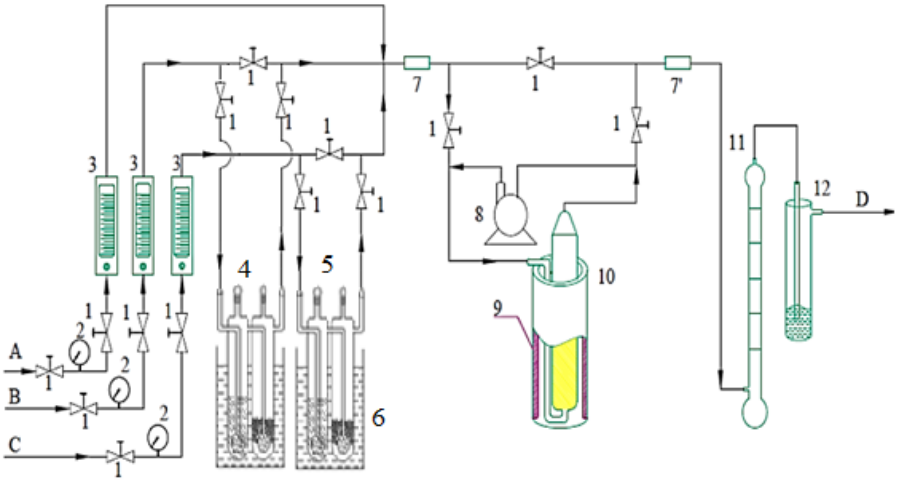

1 - Pressure regulator valve; 2 – Pressure gauge; 3 - Flowmeter ; 4 - Water tank; 5 - p-xylene tank; 6 - Thermostat; 7.7' - Sampling positions; 8 - Circulation pump; 9 - UV-LED lamp; 10 -

Thin film reactor; 11 - Flow rate metter; 12 - Exhaust gas absorption water tank; A - Airflow; B - N_2 flow, C- CO_2 flow; D - Exhaust gas flow

2.6. The kinetic study of the photocatalytic oxidation

The kinetics of the p-xylene oxidation reaction on thin films was studied by the non-gradient cyclic flow method, using mixed light (light mode I). The investigation factors are including initial partial pressure p-xylene, water vapor, oxygen, CO_2 and light intensity to reaction rate.

CHAPTER 3. PHYSICO-CHEMICAL PROPERTIES AND CATALYTIC ACTIVITIES OF THIN FILM CATALYST IN *p*-XYLENE PHOTOOXIDATION

3.1. Synthesis, characterization and photocatalytic of $LaMnO_3$

The results of the study showed that when the ratio of La:Mn = 1:1, the physico-chemical properties as well as the conversion efficiency in 60 minutes (H_{60}) reached the highest value. Therefore, in the study the perovskites are prepared with the ratio of La:Mn = 1:1.

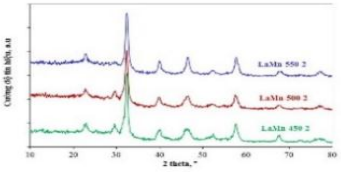

a)

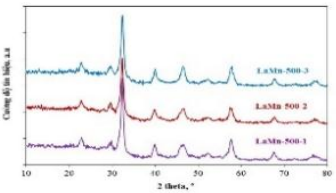

b)

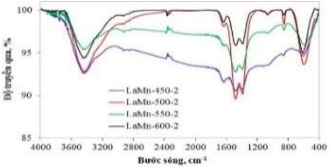

c)

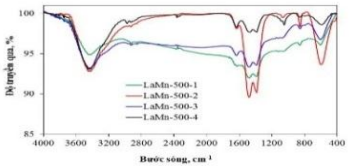

d)

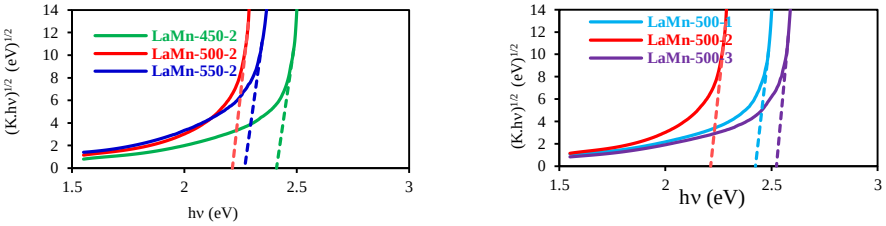

e) f)

Figure 3.1. XRD patterns (a,b), FT-IR spectra (c,d) and Tauc plot (e, f) of $LaMnO_3$ at various calcination conditions

Effects of different calcination conditions on the properties of $LaMnO_3$ were studied. The XRD patterns (Fig 3.1a, b) at various treament conditions show the formation of $LaMnO_3$ crystal lattice. When the calcination time or temperature increases, the average crystal size of $LaMnO_3$ at first increased and then decreased. The FT-IR spectra (Fig 3.1 c, d) of catalyst $LaMnO_3$ treated at various temperature showed the vibration of O-H groups at 3422 cm^{-1}, C–O at 865 cm^{-1}, Mn–O or Mn-O-Mn at 605 cm^{-1}. The Tauc plot showed $LaMnO_3$ samples can adsorp photon in visible region (λ = 490–561 nm) corresponds to the band gap energy of 1.79 – 1.95 eV.

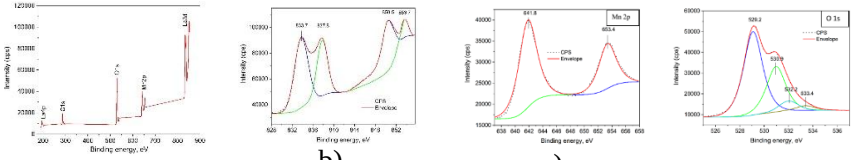

a) b) c) f)

Figure 3.2. XPS spectra of $LaMnO_3$ (a) Combination spectrum, (b) La 3d, (c) Mn 2p, (d) O 1s of $LaMnO_3$ at 500°C for 2 hrs.

The XPS spectrum of $LaMnO_3$ shows the presence of binding energies of La(3d), Fe(2p), O(1s). The XPS spectra (Fig. 3.2b, c) of La(3d) and Mn(2p) show that in $LaMnO_3$ samples, the La and Mn elements are presented in the +3 oxidation states. For O ions in the $LaMnO_3$ perovskite material including O_L: Lattice oxygen at 529.2 eV of La–O and Fe–O in the $LaMnO_3$ lattice, and oxygen in -OH group (O_H: hydroxyl oxygen) at 530.9 eV.

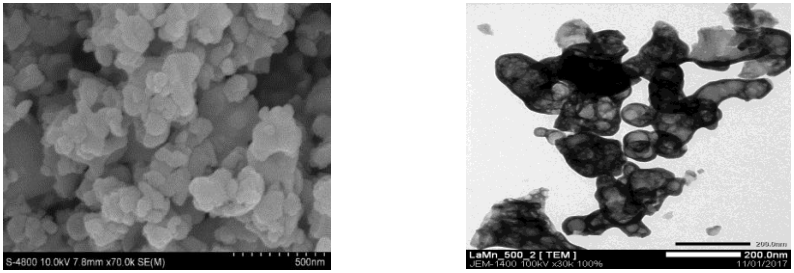

a) b)

Hình 3.3. SEM (a) and TEM (b) images of catalysts LaMn-500-2

The $LaMnO_3$ sample which was calcined at 500 ^oC in 2 hr (LaMn-500-2) has smallest crystaline size (12nm) and lowest bandgap energy (E_g = 2.21 eV) and largest wave length in visible region (λ = 561 nm) and thermal stability up to 800 ^oC. The SEM and TEM images (Fig. 3.3) show that LaMn-500-2 have the smallest crystalize size (12.0 nm) with rather uniform contribution, less clumps, so it has the highest surface area (24.8 m^2/g) and total pore volume (0.075 cm^3/g) among $LaMnO_3$ samples. The pore diameter of $LaMnO_3$ is 14 Å, larger than the molecular size of p-xylene (5.8 Å) and the average film thickness 3.8 µm is within the optimal range of thin film catalyst, eliminate the effect of slow diffusion of p-xylene reaching the innermost layer of the catalyst film.

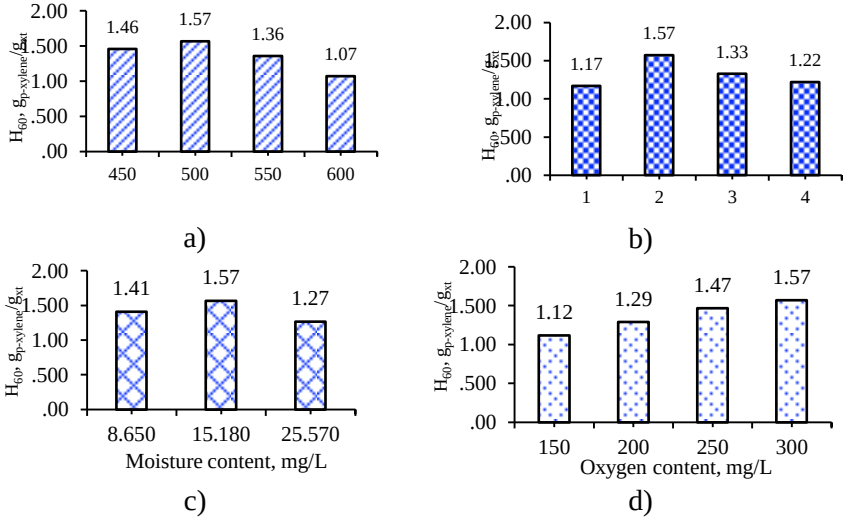

Figure 3.4. Effects of calcined temperature at 2 hr (a), calcined time at 500 ^{o}C (b), moisture content (c) and oxygen content (d) on the conversion yield of *p*-xylene H_{60} over thin film $LaFeO_3$ catalysts

Experimental results show that p-xylene is not photolysis under UV+LED light and the adsorption saturation of p-xylene on the catalyst film is set after 30 minutes with negligible amount. Figure 3.4 a,b shows that the 60-minutes-conversion efficiency of p-xylene (H_{60}) is highest when the $LaMnO_3$ catalyst is calcined at 500 ^{o}C for 2 hr. The dependence of p-xylene conversion efficiency on moisture concentration shows the maximum H_{60} value when the moisture content is 15.18 mg/L (Figure 3.4c). The decomposition efficiency of p-xylene increased with increasing oxygen content. The highest p-xylene 60-minutes-conversion efficiency of p-xylene was 1.57 g/g_{cat} at an oxygen content of 300 mg/L, equal to that of oxygen concentration in the air.

3.2. Characterization and photocatalytic of thin film $LaFeO_3$

The XRD patterns of all $LaFeO_3$ samples differenting treated conditions showed characteristic peaks of $LaFeO_3$. The sample at the calcination temperature of 500 ^{o}C for 3 hr has the smallest crystal size (9.3 nm). The Tauc plot shows that all the $LaFeO_3$ catalyst samples have low band gap energy (1.96 - 2.15 eV).

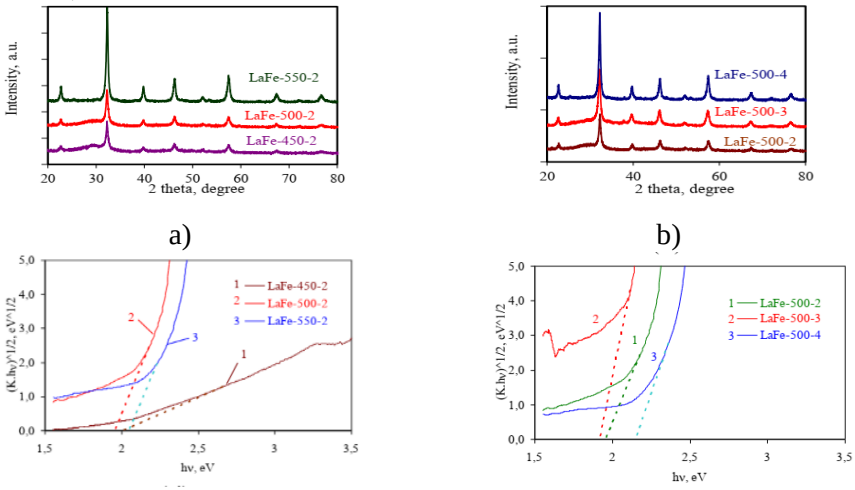

c) d)

Figure 3.5. XRD patterns (a,b) and Tauc plot (c, d) of $LaFeO_3$ at various conditions

$LaFeO_3$ sample calcined at 500 °C for 3 hr (LaFe-500-3) has the smallest band gap energy (Eg = 1.92 eV), which can be absorded Vis light with the longest absorption wavelength in the visible region (λ = 646 nm), the specific surface area (32.7 m^2/g) and the pore volume (0.127 cm^3/g) are highest.

The XPS spectrum (Fig. 3.6) of La (3d) and Fe (2p) shows that the La and Fe elements are both in the +3 valence state. For O ions in the perovskite $LaFeO_3$ showing the peak position of oxygen in the lattice (O_L: Lattice oxygen) at 528.8 eV is attributed to La–O and Fe–O in the $LaFeO_3$ lattice, and oxygen in the -OH group (OH: hydroxyl oxygen) at 531.2 eV. The average thickness of the $LaFeO_3$ catalyst film is 4.76 µm.

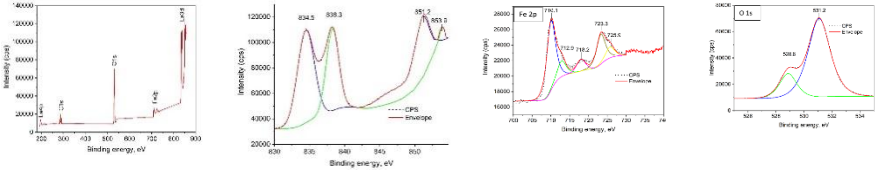

a) b) c) d)

Figure 3.6. XPS spectra of $LaFeO_3$ (a) Combination spectrum, (b) La 3d, (c) Fe 2p, (d) O 1s

Figure 3.7(a) and (b) showed that all samples with various calcination temperatures have high activities. In which, the catalyst activated at 500 ^oC in 3 hr (LaFe-500-3) showed the best physico-chemical properties, and has the highest decomposition efficiency of p-xylene. The highest *p*-xylene conversion yield was 1.70 g/g_{cat} at the moisture content of 15.2 mg/L (Fig. 3.7c).

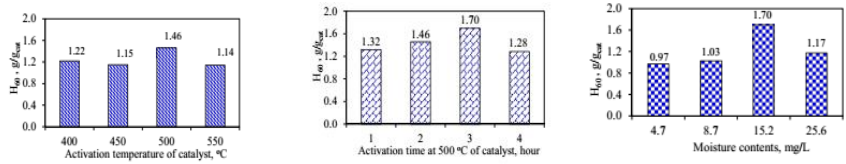

a) b) c)

Fig 3.7. Effect of calcined temperature (a), calcined time (b) and moisture content (c) on conversion yield of p-xylene H_{60} on $LaFeO_3$ thin film

3.3. Characterization and photocatalytic of thin film $LaCoO_3$

Figure 3.8 shows that the all $LaCoO_3$ obtained samples are highly crystalline with strong and clear diffraction intensity characteristic peaks of $LaCoO_3$. The average crystal size of $LaCoO_3$ changes within a narrow range (7.09 - 7.59 nm). $LaCoO_3$ has a low band gap (1.79 - 1.95 eV) and can absorb Vis light with a wavelength in the range of 636–693 nm.

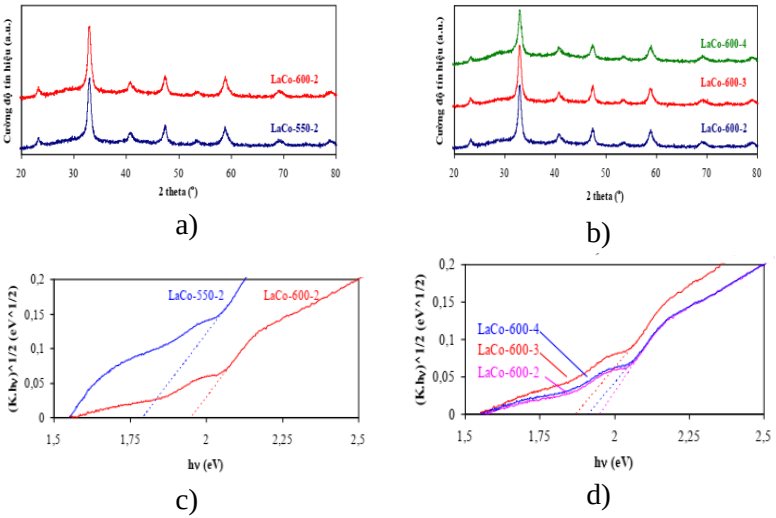

Figure 3.8. XRD patterns (a,b) and Tauc plot (e, f) of $LaCoO_3$ catalysts at various conditions

The XPS spectra (Fig. 3.9) shows the typical binding energy values of La(3d), Co(2p), O (1s), and show that La and Co ions are present in the sample in the form of M^{3+} ions.

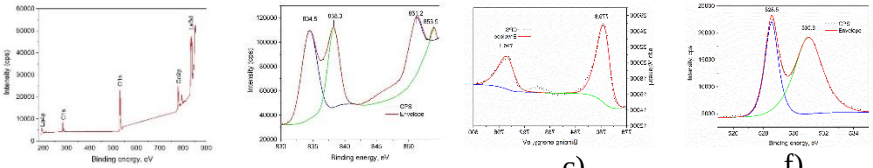

Figure 3.9. XPS spectra of $LaCoO_3$: (a) Combination spectrum, (b) La 3d,

(c) Co 2p, (d) O 1s

SEM and TEM images of $LaCoO_3$ catalysts showed the spherical particles of catalyst with particle size of about 10 - 40nm, and surface area in ranges of 17.6 - 19.9 m^2/g. Samples calcined at 600 ^oC for 3 hr had the smallest crystal size (7.59 nm) and smallest band gap energy (1.79 eV).

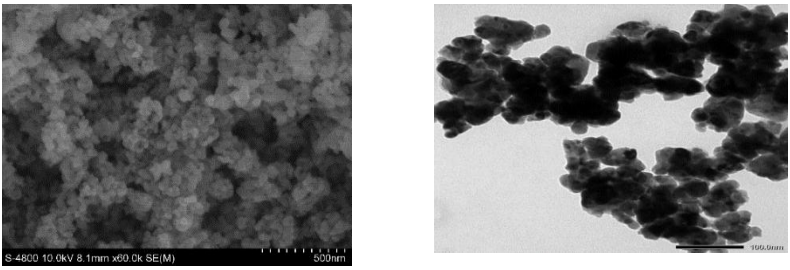

a) b)

Figure 3.10. SEM (a) and TEM (b) images of catalysts LaCo-600-3

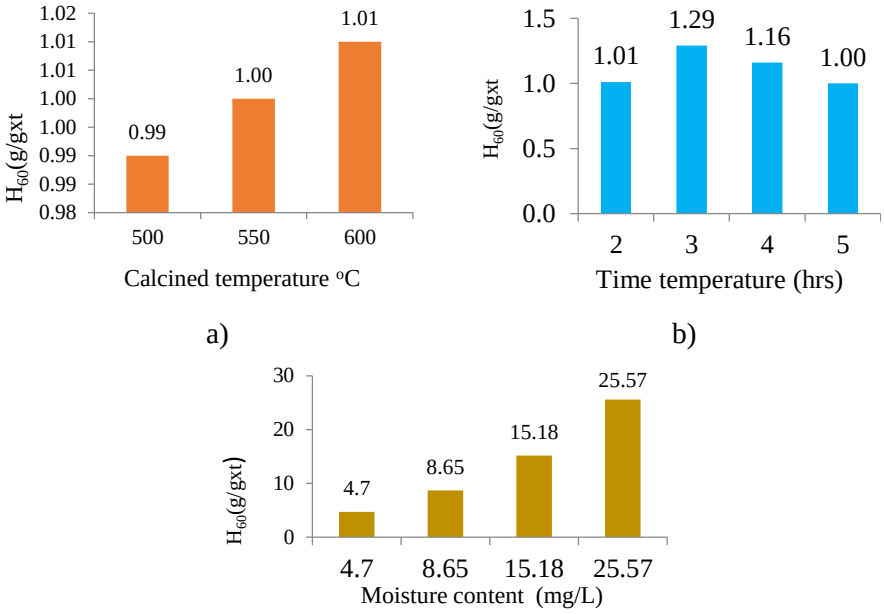

*Figure 3.11***.** Effect of calcined temperature (a); calcined time (b) and

moisture content c) on the conversion efficiency of p-xylene H_{60} on $LaCoO_3$ thin film

Figures 3.11a,b show that the $LaCoO_3$ catalyst calcined at 600 ^oC for 3 hr has a higher p-xylene conversion efficiency than the catalyst treated at other conditions. Figure 3.11c shows that the suitable moisture content for photoreaction on LaCo catalyst is 15.2 mg/L for the conversion yield H_{60} = 1.29 g/g_{cat}.

3.4. Synthesis, characterization and photocatalytic of UiO-66-NH_2 and UiO66

The investigation of effect of reaction time and amount of DMF solvent showed that UiO-66 and UiO66-NH_2 crystals have good crystallinity with the reaction time 36 hr and a solvent volume of 15 ml. The XRD pattern (Fig. 3.12a, a') shows the successful preparation of UiO66 and UiO66-NH_2 crystals with an average crystal size of 29.4 nm. UiO66 crystals have a spherical shape, size in range of 50-100 nm, and the specific surface area of UiO66 of 788.5 m^2/g. UiO-66 has a band gap of 3.01 eV and absorbs photons with a wavelength of 412 nm.

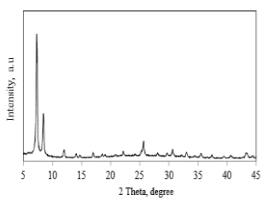

(a)

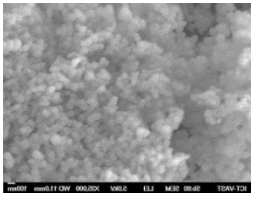

(b)

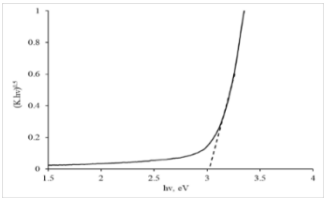

(c)

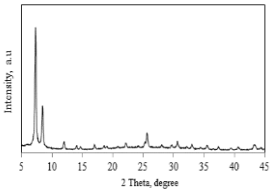

(a')

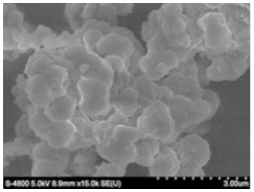

(b')

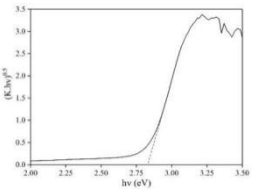

(c')

Figure 3.12. XRD pattern, SEM image and Tauc plots of UiO66 (a,b,c) and UiO66-NH_2 (a',b',c')

Sample UiO66-NH_2 has similar morphology to UiO66 as spherical crystal, but larger size (~200 nm), and smaller of specific surface area (600.8 m^2/g) and pore volume (0.302 cm^3/g). However, the band gap energy of UiO66-NH2 (2.83 eV) is smaller and longer wavelength absorption (438 nm) as compared to UiO66. The TGA analysis shows that UiO66 is stable to 423 ^oC and UiO66-NH_2 is stable to 400 ^oC. With high thermal stability, the structure of the two MOF materials will be not destroyed at the activation temperature of 200 ^oC. The average film thickness is 4.2 m, which is within the optimal range.

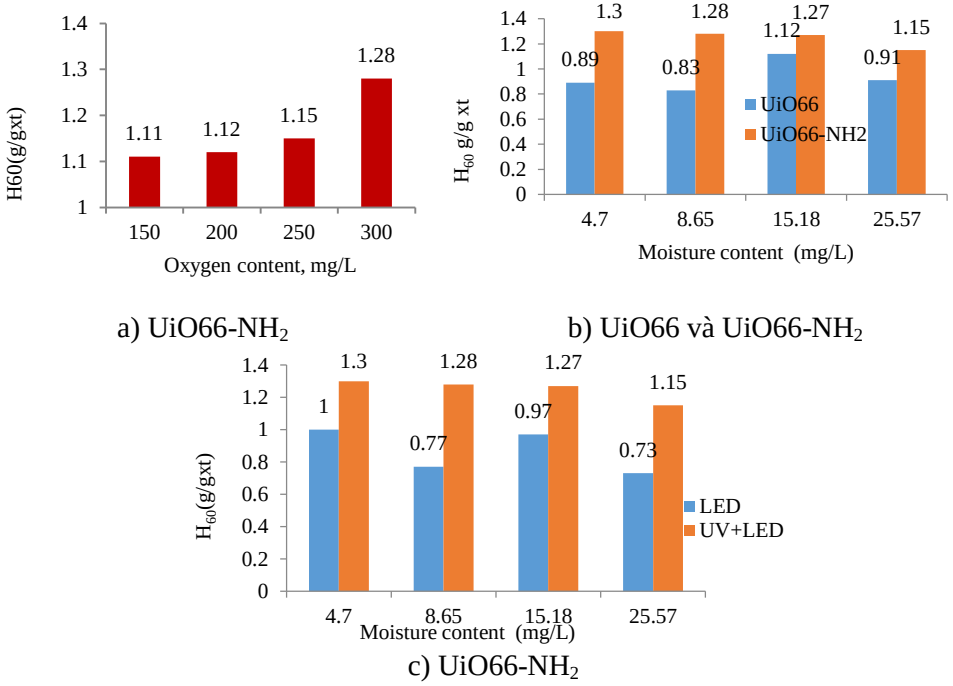

Figure 3.13. Effect of oxygen content (a), moisture contents (b) and lighting modes (c) on the conversion yield of *p*-xylene H_{60} over UiO66-NH_2 and UiO66 catalysts

Fig. 3.13a shows that the decomposition efficiency of p-xylene H_{60} was highest at the oxygen content of 300 mg/L. The highest H_{60} conversion yield was 1.12 g/g_{cat} on UiO66 catalyst at moisture content of 15.18 mg/L and 1.30 g/g_{cat} on UiO66-NH_2 at moisture content of 4.7 mg/L (Fig. 3.11b). Fig. 3.13c shows that using UV+LED combined light significantly increases *p*-xylene decomposition efficiency compared to visible light (H_{60} = 1.30 g/g_{cat} compare to 0.97 g/g_{cat}).

3.5. Photo catalyst based on Zn-MOF-74+TiO_2

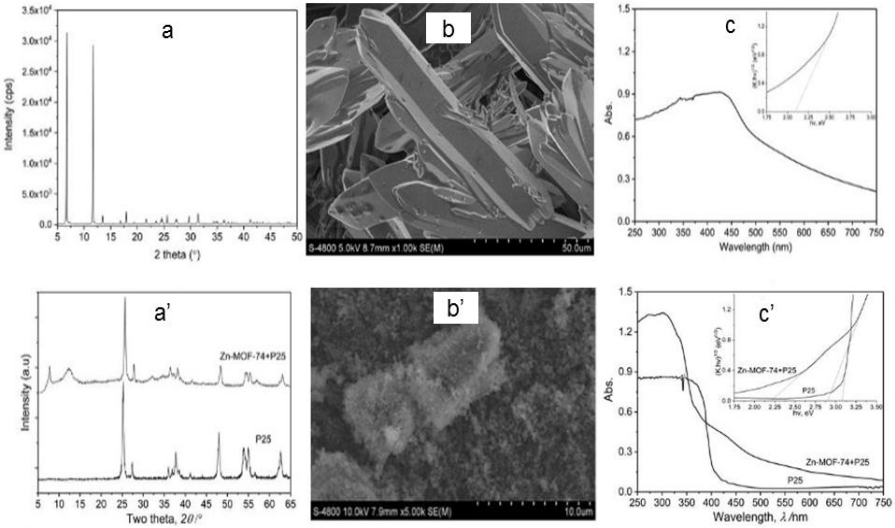

Figure 3.14. XRD pattern, SEM image and Tauc plots of Zn-MOF-74 (a, b, c) and Zn-MOF-74+TiO_2 (a', b', c')

The investigated results determined that Zn-MOF-174 crystals with good crystallinity (Fig. 3.14a) were synthesized when the reaction time was 22 hr, solvent volume of 20 mL and activated under vacuum at 250 ^{0}C for 6 hr. The average crystal size of Zn-MOF-74 is 87.5 nm. FT-IR spectra show that that the free DMF molecules have been completely removed after activation and Zn-MOF-74 crystal was obtained. Synthesized Zn-MOF-174 has a specific surface area of 826 m^2/g, pore volume of 0.344 cm^3/g, pore diameter of 1.42 nm. The

UV-Vis spectrum (Fig. 3.14c) shows that Zn-MOF-74 absorbs visible light with a light wavelength of about 594 nm, corresponding to a band gap energy (Eg) of 2.09 eV. Crystalline Zn-MOF-74 has a long, sharp rod shape, micrometer size (2.5-10) µm x (30- 80) µm (Fig. 3.14b), making it difficult to create thin films on glass tube. To overcome this difficulty the TiO_2 P25 of 30 nm particle size was added into the Zn-MOF-74 solution as a binder.

The XRD pattern (Fig. 3.14a') of the mixed Zn-MOF-74 + TiO_2 sample show the crystal phase composition of Zn-MOF-74 and TiO_2 P25. Compared to the pure Zn-MOF-74, the crystal size of Zn-MOF-74 +TiO_2 reduces from 87.5 nm to 75.0 nm, while the that of P25 reduced from 35.0 nm to 23.6 nm. In the composite material, the long rod-shaped crystalline of Zn-MOF-74 are covered with small-sized P25 particles (20-25 nm) (Fig. 3.14b'). The Zn-MOF-74+TiO_2 composite material absorbs photons at 428 nm corresponding to a band gap energy of 2.90 eV (Fig. 3.14c'), smaller than P25 (3.08 eV), but bigger than that of the Zn-MOF-74 (2.09 eV). Thin films of Zn-MOF-74 + P25 composite materials were successfully fabricated with a small film thickness of about 2.6 µm.

The conversion yield of the Zn-MOF-74+TiO_2 sample with the weight ratio 2:1 reached 1.25 g/g_{xt}, which was much higher than the other ratios (Fig. 3.15a). On Zn-MOF-74+TiO_2, with the most suitable moisture content of 8.65 mg/L. The use of combined UV-LED light has been improved the *p*-xylene conversion yield (H_{60}) compare to LED light (1.25 compare to 1.07 g_x/g_{cat}).

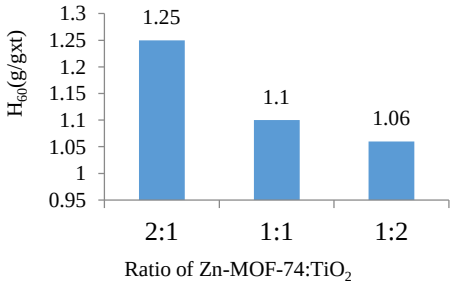

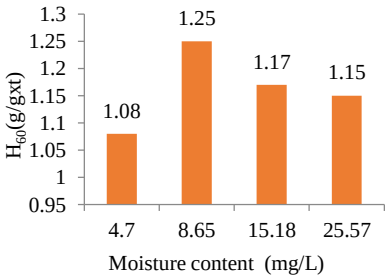

a) b)

Figure 3.15. Conversion yield of p-xylene H_{60} on Zn-MOF-74+P25 with: a) different ratio of Zn-MOF-74/TiO_2, and b) different moisture content

3.6. *Comparison of properties and activities of the best catalysts*

Table 3.1. Average crystal size (d_{crys}), average particle size (d_{par}), specific surface area (S_{BET}), pore volume (V_{por}), pore size (d_{por}), band gap energy (E_g), light absorption edge (λ), thickness of thin film (δ), initial conversion (X_o) and 60-min removal efficiency (H_{60}) of the best catalyst sample under mixture light mode UV-Vis (I)

Catalysts	d_{crys}, nm	d_{par}, nm	S_{BET}, m^2/g	V_{por}, cm^3/g	d_{por}, Å	E_g, eV	λ, nm	δ, μm	X_o, %	H_{60}, g_{xyl}/g_{xt}
$LaFeO_3$	9.3	8-15	32.7	0.127	5.2	1.92	646	4.7	100	1.70
$LaMnO_3$	12.1	15–35	24.8	0.075	2.8	2.2	561	5.1	87.5	1.57
$LaCoO_3$	7.6	10–40	17.6	0.065	8.4	1.87	663		72.9	1.29
UiO66	29.4	50–100	788.5			3.01	412		57.3	1.12
UiO66-NH_2	35.0	100–200	600.8	0.302	1.9	2.83	438	4.2	95	1.30
Zn-MOF-74	87.5	2500-10000	826	0.344	1.4	2.09	594			
Zn-MOF-74 +P25	75.0		90.3	0.277		2.90	428	2.6	64.0	1.25
P25	35	30	42.5	0.04	2.5	3.08	403	2.75	29.0	-

The results from Table 3.1 show that the thin film photocatalysts based on perovskites and MOFs have been successfully prepared with high crystallinity. Most of the prepared catalysts have low bandgap energies, in the optimum range

(2.2 – 3 eV) and absorb visible light (λ ≥ 412 nm), film thickness (2.6–5.1μm) within the optimum range for thin film of photocatalyst. The catalysts have high p-xylene treatment efficiency. The perovskite catalysts have low band gap energy, while MOF catalysts have high specific surface area. Under the most suitable reaction conditions, the activities of the catalysts can be arranged in the following order: $LaFeO_3$ > $LaMnO_3$ > UiO66-NH_2 > $LaCoO_3$ > (Zn-MOF-74 +P25) > UiO66 > P25. Three catalysts $LaFeO_3$, $LaMnO_3$, UiO66-NH_2 had the highest p-xylene photooxidation activity with initial conversion of 88-100% and H_{60} treatment efficiency of 1.3 - 1.7 g/g_{cat}. These typical catalysts have higher photodegradation activity of p-xylene than the commercial TiO_2 Degusa P25 catalyst.

3.7. Kinetic of p-xylene photooxidation reaction on $LaFeO_3$ and UiO-66-NH_2 thin films

From the above study, possessing mesoporous structure and low band gap energy (1.92 và 2.83 eV) perovskites $LaFeO_3$ and UiO-66-NH_2 exhibited highly active and stable for the gas phase photodegradation of p-xylene under the radiation of combined UV + Vis lights. So, the kinetics of photocatalytic degradation of *p*-xylene was studied on UiO-66-NH_2 and $LaFeO_3$ thin films under combined illumination of UV + Vis (lights the irradiation mode I).

It was reported that due to the optimal thickness of thin film (4.2-4.7 μm) and large the pore diameter (1.9 và 5.2 nm) the internal diffusion effect is excluded. The reaction was carried out under experimental conditions, which excluded the influence of external diffusion. Thus, the reaction takes place in the kinetic region. The law of influence of reaction conditions on the reaction rate is summarized in Fig. 3.16.

The the dependence convex curve of the p-xylene conversion rate (r) on the partial pressure of p-xylene (P_{xyl}) (Fig. 3.16a) shows that the quantity P_{xyl} is present in both the numerator and the denominator of the kinematics equation. On the UiO66-NH_2 catalyst (Fig. 3.16b), the reaction rate depends on the

oxygen concentration in the form of a concave curve, while on the $LaFeO_3$ catalyst, it has a line through the extreme point, that means on both digital catalysts the oxygen concentration term is involved both in the numerator and denominator of the kinetic equation, where on the $LaFeO_3$ catalyst the order in the denominator must be higher than in the numerator. The extreme dependence of r on P_{H2O} (Fig. 3.16c) shows that moisture pressure is present in both the numerator and denominator of the kinetic equation, with the exponent in the denominator being higher than the value in the numerator. The almost linear dependence of the reaction rate inversion (1/r) on the CO_2 content (Fig. 3.16e) shows that the partial pressure of CO_2 participates in the denominator of the kinetic equation with an exponent of 1. Fig. 3.16d shows that the photon flux is present on the numerator of the kinetic equation in the form of Φ^{β}.

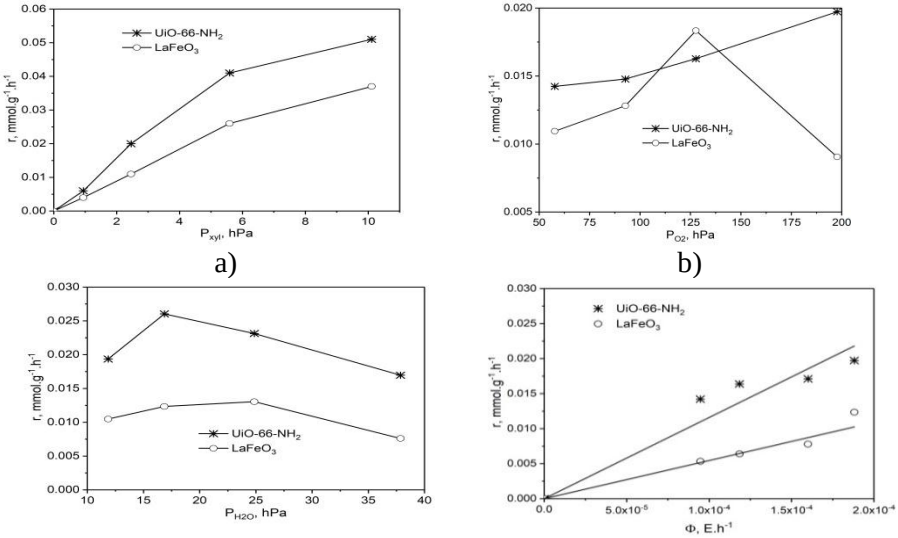

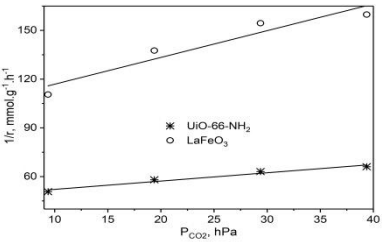

e)

Figure 3.16. The dependence of the reaction rate (r) on the partial pressures of a) p-xylene (P_{xyl}); b) oxygen (P_{O2}), c) moisture (P_{H2O}), d) the light flux (Φ), and e) the inverse reaction rate (1/r) on the partial pressures of CO_2 (P_{CO2})

Therefore, the kinetic equation for the oxidation of p-xylene on the two catalysts UiO-66-NH_2 and $LaFeO_3$ has the following general form:

$$r = \frac{kP_{xyl}^{n_1}(k_1P_{O_2}^{n_2} + k_1^{'}P_{H_2O}^{n_3})\phi^{\beta}}{(1 + k_2P_{xyl}^{m_1} + k_3P_{O_2}^{m_2} + k_4P_{H_2O}^{m_3} + k_5P_{CO_2}^{m_4} + + k_6P_{xyl}^{m_1}P_{H_2O}^{m_3})^{2\alpha}}$$

where r is reaction rate of p-xylene photooxidation; k is the observed rate constant; k_i are the kinetic constants; P_i are partial pressure of the corresponding components; Φ is photon flux; n_1, n_2, n_3, m_1, m_2, m_3, m_4, and β are reaction orders of the corresponding reactants and photon flux; and 2α is surface coverage.

Calculations show that the calculated data are most suitable with experimental data when the reaction kinetics is described by the following equation:

$$r = \frac{kP_{xyl}(k_1P_{O_2} + k_1^{'}P_{H_2O}^{0.5})\phi^{\beta}}{(1 + k_2P_{xyl} + k_3P_{O_2} + k_4P_{H_2O}^{0.5} + k_5P_{CO_2})^2} \qquad (3.1)$$

The kinetics of p-xylene photooxidation on P25 thin films under similar conditions and UV light are also described by Equation (3.1). The values of kinematic constants are presented in Table 3.2.

Table 3.2. The values of the kinetic constants of equation (3.1)

Kinetic constants	Unit	Catalysts		
		P25*	UiO-66-NH_2**	$LaFeO_3$**
k	$g^{-1}.h^{\beta-1}.E^{-\beta}$ $hPa^{-1}.E^{-\beta}$	1.197×10^{-2} ***	1.637	4.4490

Kinetic constants	Unit	Catalysts		
		P25*	UiO-66-NH_2**	$LaFeO_3$**
k_1	hPa^{-1}	0.639×10^{-3}	$3.51x10^{-2}$	3.4421
k_1'	$hPa^{-0,5}$	1.677×10^{-2}	1.745	3.4500
k_2	hPa^{-1}	5.078×10^{-8}	$1.00x10^{-3}$	0
k_3	hPa^{-1}	0	1.563×10^{-5}	3.95×10^{-2}
k_4	$hPa^{-0,5}$	1.00×10^{-2}	3.922×10^{-2}	3.026×10^{-1}
k_5	hPa^{-1}	0	4.888×10^{-3}	8.23×10^{-2}
k_6	$hPa^{-1,5}$	0	0	0
α		1	1	1
β		0.537	0.888	1.03
Variance	%	20.5	15.5	22.7

*) *three light UV (λ = 365 nm, 8 W/light; 650 Lux/light); **) combine UV-Vis (mode I);* ***) $g^{-1}.h^{-1}.lux^{-\beta}$

The results show that equation (3.1) following the Langmuir–Hinshelwood mechanism, is the general kinetic equation for p-xylene photooxidation on the thin film of MOF catalysts UiO-66-NH_2 and perovskite $LaFeO_3$ under combined UV-Vis lights irradiation as well as on P25 catalyst illuminated by UV light. In which the reaction between adsorbed p-xylene molecular with hydroxyl radical ($^{\bullet}OH$) formed from adsorption of steam on the photogenerated hole and adsorbed electron accepted oxygen ($^{\bullet}O_2$), is the rate-determining step. The physicochemical properties of the catalysts are shown through the difference in kinetic constants. By the shift to visible light adsorption, the photocatalysts UiO66-NH_2 and $LaFeO_3$ have higher light utilization efficiency for the main process ($\beta \sim 1$), reducing photogenic e-h^+ recombination, resulting in a higher reaction rate constant (k) than that of the TiO_2 P25 catalyst.

CONCLUSIONS AND SUGGESTIONS

CONCLUSIONS

In the thesis, two new groups of photocatalysts with low bandgap energy, activating under visible light, perovskite and MOF, have been successfully

prepared and used in the treatment of VOC polluted gas, representative by p-xylene.

1. The best conditions to synthesize perovskite with the most outstanding properties have been determined. Ratio of precursor La nitrate:M nitrate is 1:1; suitable calcination temperature for $LaMnO_3$ and $LaFeO_3$ is 500^oC, while for $LaCoO_3$ is 600^oC; suitable calcination time for $LaMnO_3$ is 2 hours and 3 hours for the other two perovskites. The perovskites have high crystallinity and purity, low band gap energy (1.87–2.21 eV), absorption and activation by visible light (λ=561-663 nm) and high specific surface area. $LaCoO_3$ has the smallest crystal size (~8 nm) and the lowest bandgap energy (1.87 eV), the longest light absorption (λ= 663 nm), but has the smallest specific surface area (17.6 m^2/g). $LaFeO_3$ has the largest specific surface area (32.7 m^2/g), and second place in terms of crystal size (~10 nm) and band gap energy (1.92 eV) with absorption wavelength (λ = 646 nm). $LaMnO_3$ has the largest crystal size (12 nm), the highest band gap energy (2.21 eV), but is still within the optimal range, and has the shortest absorption wavelength of 561 nm and a relatively high specific surface area (26 m^2/g).

2. The photocatalysts UiO66, UiO66-NH_2 and Zn-MOF-74 have been successfully prepared by solvo-thermal method. Under suitable synthesis conditions in this study, the prepared MOFs have high crystallinity, low band gap energies of 3.01 eV, 2.83 eV and 2.9 eV, respectively, and absorb visible light (λ = 412 - 594 nm), that can be a visible photocatalyst. The outstanding advantage of this group of catalysts is that it has a large surface area, 1045 m^2/g, 873 m^2/g and 826 m^2/g for UiO66, UiO66-NH_2 and Zn-MOF-74, respectively.

3. Successfully fabricated thin film catalysts on pyrex glass tubes from perovskite $LaMO_3$, UiO66, UiO66-NH_2 and a mixture of Zn-MOF-74 + TiO_2 P25 by dip-coating method with thickness of 2.6–5.1 μm, being within the optimum value (2-8 m), which favors light absorption and catalyst diffusion,

leading to high photocatalytic activity, although the amount of catalyst used is very small (15 mg).

4. The suitable conditions for high catalyst efficiency in photodegradation of p-xylene have been determined (moisture concentration, O_2 concentration and the mixed UV-Vis light). In the mixed UV-Vis illumination mode, the photoactivity of the synthetic perovskite and MOF catalysts is much higher than that of the commercial TiO_2 P25 and the activity was aranged in follow order: $LaFeO_3$ > $LaMnO_3$ > UiO66-NH_2 > $LaCoO_3$ > Zn-MOF-74 +P25 > UiO66 >> TiO_2 P25.

5. The reaction kinetic was comprehensively studied and based on the dependence of the reaction rate on the influencing factors the kinetic equation has been proposed. The kinetics of photocatalytic degradation of *p*-xylene under combined illumination of ultraviolet and visible lights over obtained UiO-66-NH_2 and $LaFeO_3$ thin films as well on TiO_2 P25 under UV light has the following form and follows Langmuir–Hinshelwood model

$$r = \frac{kP_{xyl}(k_1P_{O_2} + k_1^{'}P_{H_2O}^{0.5})\phi^{\beta}}{(1 + k_2P_{xyl} + k_3P_{O_2} + k_4P_{H_2O}^{0.5} + k_5P_{CO_2})^2}$$

Thank to the extension of light adsorbtion to the visible region, the UiO-66-NH_2 and $LaFeO_3$ catalysts have a higher light utilization efficiency, resulting in a higher reaction rate constant and photoactivity than TiO_2 P25.

Perovskite and MOF semiconductors with low bandgap energies are highly active under visible light. The study opens up the possibility of applying perovskite and MOF as sunlight-activated photocatalysts for purifying polluted gas.

SUGGESTIONS

1) To develop and diversify perovskite- and MOF- based photocatalysts for environmental cleaning under natural conditions.

(2) To improve treatment efficiency of perovskite- and MOF-based photocatalysts by modification with new and diverse ways.

(3) Expanding the application of perovskite and MOF for the treatment of other waste gases such as benzene, methane, etc. and organic compounds in the liquid phase in order to create photocatalyst technology to treat polluted environment using sunlight.

NEW CONTRIBUTIONS OF THE THESIS

In this thesis the visible light photocatalysts including $LaMO_3$ (M: Mn, Fe, Co) and MOFs (UiO66-NH_2, Zn-MOF-74) have been successfully prepared by sol-gel and solvent-thermal methods, respectively. The results show that combining UV with visible light is an effective measure to both improve the efficiency of pollutant treatment and create a scientific basis for the use of sunlight. The prepared $LaMO_3$ and MOFs catalysts show higher photodegradation activity for *p*-xylene degradation in polluted gas than commercial TiO_2 P25, which are potential new catalysts for development and application in sunlight-based technology for exhaust gas treatment in natural conditions. The preparation and using of catalyst is in thin film form facilitate easy recovery and reuse, limit secondary pollution, and facilitate expanding practical applications.

The photo kinetic of p-xylene decomposition in the gas phase on perovskite and MOF catalysts using UV-Vis combination light is a new issue. The results of the study of kinetics and reaction mechanism provide a deep insight of the nature of the process and thus provide precise directions in improving and enhancing the catalytic activity and also acting as a connection between basic research in the laboratory with reactor design and implementation. This thesis was also solved the above problems in parallel will contribute to the introduction of photocatalytic technology to volatile organic matter treatment under natural conditions, using sunlight and saving energy.

LIST OF PUBLICATIONS

Domestic journal papers

1. Luu Cam Loc, Nguyen Thi Thuy Van, Nguyen Thi Cam Luyen, Bui Thi My Nuong, Nguyen Tri, Nguyen Phung Anh, Hoang Tien Cuong (2017), "Photooxidation of *p*-xylene on thin film $LaFeO_3$ perovskite", *Vietnam Journal of Chemistry*, 55, 3e, 92–97.
2. Loc L. C., Van N. T. T., Huynh N. H., Tri N., Kieu P. T. P., Cuong H. T., Anh H. C. (2017), $UiO66\text{-}NH_2$ as a new photocatalyst for the degradation of *p*-xylene in gaseous phase, *Journal of Science and Technology*, 55, 1B,40-48.
3. Nguyễn Thị Thùy Vân, Lưu Cẩm Lộc, Nguyễn Trí, Hoàng Tiến Cường, Nguyễn Thị Cẩm Luyến, Trần Thanh Lực, Hoàng Khánh Vũ, Hà Cẩm Anh, Quang xúc tác phân hủy *p*-xylene ở pha khí trên màng mỏng $LaCoO_3$, Tạp chí hóa học, 55, 5e34, 176-180, 2017

International journal papers

1. Cam Loc Luu, Thi Thuy Van Nguyen, Tri Nguyen, Phung Anh Nguyen,Tien Cuong Hoang and Cam Anh Ha, Thin film nano-photocatalyts with low band gap energy for gas phase degradation of p-xylene: TiO_2 doped Cr, $UiO66\text{-}NH_2$ and $LaBO_3$ (B = Fe, Mn, and Co), Adv. Nat. Sci.: Nanosci. Nanotechnol. 9 (2018) 015003 (8pp), https://doi.org/10.1088/2043-6254/aa9db1
2. Van Nguyen Thi Thuy, Loc Luu Cam, Tri Nguyen, Anh Nguyen Phung, Anh Ha Cam, Tinh Nguyen Thanh, Duong Nguyen Lam Thuy, Cuong Hoang Tien, Kinetics of photocatalytic degradation of gaseous *p*-xylene on $UiO\text{-}66\text{-}NH_2$ and $LaFeO_3$ thin films under combined illumination of ultraviolet and visible lights, *Int. J. Chem. Kinet.* 2019;1–17., DOI: 0.1002/kin.21328
3. Van Thi Thuy Nguyen, Cam Loc Luu, Tri Nguyen, Anh Phung Nguyen, Cuong Tien Hoang and Anh Cam Ha, Multifunctional Zn-MOF-74 as the gas adsorbent and photocatalyst, Adv. Nat. Sci.: Nanosci. Nanotechnol. 11 (2020) 035008 (11pp).

Conference

1. Luu Cam Loc, Nguyen Thi Thuy Van, Bui Thi My Nuong, Tran Thanh Luc, Bui Thanh Hau, Nguyen Tri, Ha Cam Anh, Hoang Tien Cuong, *Photocatalytic activity of $LaMnO_3$ thin film in degaration of p-xylene in gaseous phase under UV – LED irradiation*, Proceedings of the 6^{th} Asian symposium on advanced Materials, *Ha Noi, Viet Nam*, 2017, 715–7